

Quasiparticle band-edge energy and band offsets of monolayer of molybdenum and tungsten chalcogenides

Yufeng Liang,¹ Shouting Huang,¹ Ryan Soklaski,¹ and Li Yang¹

¹*Department of Physics, Washington University in St. Louis, St. Louis, MO 63130, USA*

(Dated: November 8, 2018)

Abstract

We report the quasiparticle band-edge energy of monolayer of molybdenum and tungsten dichalcogenides, MX_2 ($\text{M}=\text{Mo}, \text{W}$; $\text{X}=\text{S}, \text{Se}, \text{Te}$). Beyond calculating bandgaps, we have achieved converged absolute band-edge energies relative to the vacuum level. Compared with the results from other approaches, the GW calculation reveals substantially larger bandgaps and different absolute quasiparticle energies because of enhanced many-electron effects. Interestingly, our GW calculations ratify the band-gap-center approximation, making it a convenient way to estimate band-edge energy. The absolute band-edge energies and band offsets obtained in this work are important for designing heterojunction devices and chemical catalysts based on monolayer dichalcogenides.

PACS numbers:

Recently, two-dimensional (2D) semiconducting monolayer and few-layer dichalcogenides have drawn significant interest from researchers in light of the materials' exciting chemical, electrical, and optical properties [1–9]. For example, enhanced spin-orbital coupling and unique optical selection rules make these materials promising for spintronics applications [10–13]. Accordingly, the electronic structure and, in particular, the quasiparticle energy of 2D dichalcogenides have been intensively studied to date. It is of particular interest that first-principles GW calculations have shown that enhanced many-electron effects dictate bandgaps of these 2D semiconductors [15, 16].

However, many important properties of semiconductors are not solely decided by the bandgap. For instance, the relative band-edge energies between different semiconductors and corresponding band offsets are of fundamental interest in solid state physics and are indispensable for the design of heterojunction devices [18–20]. Dichalcogenides have been known catalysts for years [7–9, 21]. Understanding the ways in which quantum confinement modifies the absolute band-edge energy and associated charge-transfer processes of chemical reactions in these monolayer or few-layer semiconductors is of critical importance for their catalytical applications. Recently, substantial advances have been achieved in obtaining qualitative band offsets [22, 23], but there has been extremely limited progress towards overcoming the bandgap problem and including enhanced many-electron effects in order to achieve accurate quasiparticle energies in monolayer dichalcogenides .

Here we employ the well-established first-principles GW approach to solve the aforementioned problems. Usually obtaining the absolute band-edge energy and band offsets of semiconductors requires, at least, two conditions: 1) a reference energy level and 2) an accurate quasiparticle energy. Because we are considering isolated samples of these 2D dichalcogenides, it is natural to choose the surrounding vacuum as the reference energy. The more sophisticated challenge, however, is obtaining the quasiparticle energy. In particular, we must ensure that the absolute energies are well-converged; this process is significantly more costly than is the bandgap calculation [24, 25]. In this vein, approximations that estimate the absolute band-edge energy but avoid a fully-converged GW calculation have been proposed [26] but their validity has not yet been verified in dichalcogenides. Given this context, the simple atomic structures and relatively inexpensive cost of fully-converged GW calculations for monolayer dichalcogenides make these systems excellent vehicles for obtaining reliable absolute band-edge energies and, moreover, ratifying the aforementioned

approximations.

In this study, our calculation provides the quasiparticle energy and corresponding band offsets of monolayer dichalcogenides via the single-shot G_0W_0 calculation. The enhanced many-electron interactions in such confined 2D semiconductors significantly enlarge the bandgap and change the absolute band-edge energy accordingly. The absolute band-edge energy and band offsets from the GW calculation are substantially different from those of density functional theory (DFT) and hybrid functional theory (HFT). On the other hand, the types of band alignments from DFT and HFT qualitatively agree with the GW results, meaning DFT and HFT are valuable for band-alignment estimations, especially given their inexpensive simulation costs. Interestingly, we find that the band-gap-center model gives a surprisingly accurate absolute band-edge energy without requiring a converged GW calculation. Ultimately, the absolute quasiparticle band-edge energies and band offsets obtained in this work will be helpful for designing heterojunctions and catalysts comprised of these materials.

We apply the generalized gradient approximation (GGA) of Perdew-Burke-Ernzerhof (PBE) as the exchange-correlation functional in the DFT calculation [27]. The single-shot G_0W_0 calculation is employed to obtain the quasiparticle energy. The spin-orbital coupling is not considered in this study. The plane-wave cutoff for the DFT calculation is set to be 80 Rys. The norm-conserving pseudopotentials [28] of molybdenum and tungsten include the 4s4p and 5s5p semi-core electrons, respectively. The k-point sampling is 12x12x1 for both DFT and GW calculations. The dielectric-function energy cutoff is set to be 10 Rys and the generalized plasmon-pole model (GPP) is applied to obtain the dynamical screening [29]. A slab Coulomb truncation is applied to mimic the isolated monolayer structure with a vacuum spacing of 23 Å between adjacent layers. All structures are fully relaxed according to the force and stress by the DFT/PBE calculation. Their relaxed lattice constants, listed in Table I, are well consistent with previous results [15, 22].

The general features of the band structures of studied monolayer molybdenum and tungsten dichalcogenides are similar. As an example, we plot the bandstructure of MoS_2 , which exhibits a direct bandgap, via DFT calculation in Fig. 1. As revealed by many other works, there is another local maximum of the valence band at the Γ point, whose energy is very close to the valence band maximum (VBM) at the K point. Interestingly, this local maximum at the Γ point will increase to become the VBM in few-layer MoS_2 and thus the overall

TABLE I: Structure and electronic properties of calculated monolayer dichalcogenides: lattice constant a , band gap E_g , the energy difference Δ_v and Δ_c defined in Fig. 1. (The HSE result is read from Reference 22.)

	a (Å)	E_g^{DFT} (eV)	E_g^{HSE} (eV)	E_g^{GW} (eV)	Δ_v^{DFT} (eV)	Δ_v^{GW} (eV)	Δ_c^{DFT} (eV)	Δ_c^{GW} (eV)
MoS ₂	3.18	1.69	2.02	2.75	0.02	0.16	0.25	0.23
MoSe ₂	3.31	1.43	1.72	2.33	0.23	0.34	0.23	0.33
MoTe ₂	3.51	1.10	1.28	1.82	0.59	0.83	0.15	0.34
WS ₂	3.20	1.78	1.98	2.88	<0.002	0.06	0.25	0.25
WSe ₂	3.33	1.50	1.63	2.38	0.26	0.34	0.21	0.36
WTe ₂	3.52	1.10	1.03	1.77	0.65	0.79	0.45	0.39

band structure turns out to possess an indirect bandgap, which dramatically changes the photoluminescence. [3]

In order to track the change of this subtle but important change in band structure, we denote the energy difference as Δ_v , which is marked in Fig. 1, and list its values in Table I. For most monolayer dichalcogenides, Δ_v^{DFT} is positive and larger than 20 meV. The only exception is WS₂, whose Δ_v^{DFT} is almost zero. However, the further inclusion of the spin-orbital coupling usually increases the VBM at the K point [22], preserving monolayer WS₂ as a direct bandgap semiconductor. Moreover, from Table I, we can see that the value of Δ_v^{DFT} increases as the group-VI element of dichalcogenides changes from S, Se, to Te. Meanwhile, we have marked the energy difference, Δ_c , between the lowest conduction band at the K point, which is the CBM, and that at the Σ point. The corresponding data are also listed in Table I. At the DFT level, Δ_c is around a few hundreds meVs for all studied monolayer dichalcogenides.

Having applied the single-shot G_0W_0 approach to calculate the quasiparticle energy of those six monolayer dichalcogenides, the results are summarized in Table I. First, the GW correction significantly enlarges the bandgap for all studied dichalcogenides. This enhanced many-electron effect has been widely observed in many reduced dimensional semiconductors as a result of depressed screening and stronger electron-electron ($e-e$) interactions [30, 31, 33]. Our GW calculated bandgaps are in good agreement with previous results [15, 16].

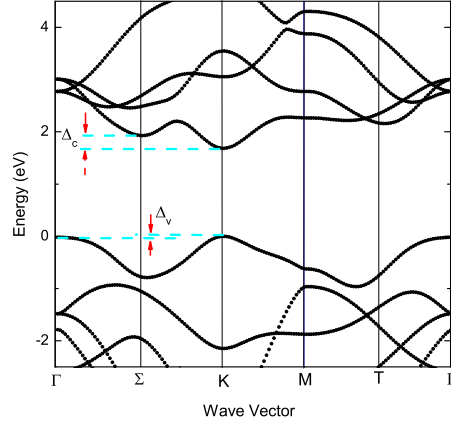


FIG. 1: (Color online) DFT-calculated band structure of monolayer MoS2. The top of valence band is set to be zero. The energy difference between the conduction band minimum at the K point and the local minimum at the Σ point is denoted by Δ_c . The energy difference between the valence band maximum at the K point and the local maximum at the Γ point is denoted by Δ_v .

Meanwhile, we have listed the bandgaps as calculated by HFT with the HSE functional [14] read from Ref. [22]. It can be seen that the GW bandgaps are significantly larger than those from HFT/HSE.

From Table I, one can see that the direct bandgap feature is preserved for all of our calculated monolayer dichalcogenides: the signs of all energy differences, Δ_v and Δ_c , remain unchanged after GW corrections. We find that the inclusion of the 4s and 5s semi-core electrons is crucial for preserving the direct bandgap feature in the GW calculation; otherwise, the local minimum of the lowest conduction band at the Σ point would be the CBM, resulting in an indirect band gap. Our result is also slightly different from another previous work, in which an indirect bandgap of the WSe₂ structure is observed. [15] This difference could be from the spin-orbital coupling.

Beyond the quasiparticle bandgap, we have calculated the absolute band-edge energy relative to the vacuum level [23, 25]. The absolute band-edge energy at the DFT level is referred to the vacuum level that is defined by the potential energy in the vacuum between dichalcogenide monolayers in our supercell arrangement, as shown in Fig. 2. Then we pre-

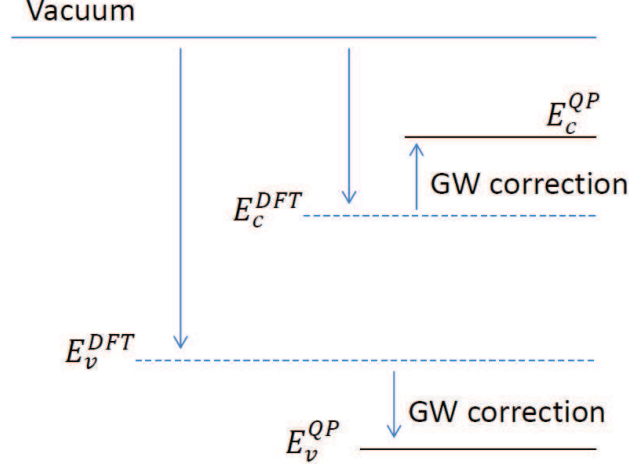


FIG. 2: (Color online) Schematic illustration of the absolute band energy at the DFT and GW levels, respectively, relative to the vacuum level.

form the GW calculation and superpose the self-energy corrections to the DFT eigenvalues, obtaining the absolute quasiparticle energy relative to the vacuum level. In Fig. 2, the final absolute quasiparticle band-edge energies are E_c^{QP} and E_v^{QP} for the CBM and VBM, respectively.

Unlike the bandgap calculation, the convergence of the absolute quasiparticle band-edge energy with respect to the number of unoccupied conduction states included in the self-energy calculation is very slow. For example, we present the convergence of the CBM and VBM of monolayer MoS₂ in Fig. 3. Although the quasiparticle bandgap is reasonably converged at a value of 2.75 eV after including around 200 conduction bands, the absolute values of CBM and VBM do not reach their converged values until we include around 1500 conduction bands.

In order to understand the slow convergence of the absolute quasiparticle energy, we must examine the details of self-energy in the GW calculation. Usually, the self-energy correction is comprised of two contributions according to their physical origins, the Coulomb-hole (COH) term and the screened-exchange (SEX) term [29]. The aforementioned slow convergence is mainly due to the COH term that involves the summation of an infinite number of conduction bands, in principle [29]. We find that the SEX term also converges slowly, although it is faster than the COH term. Thus we use around 500 conduction bands for the calculation of the static screening and around 1500 conduction bands for the final self-energy calculation.

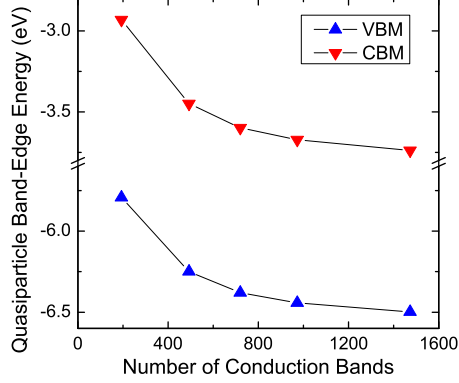


FIG. 3: (Color online) The convergence of the quasiparticle energy of the CBM and the VBM, respectively, according to the number of conduction band included in the GW calculation.

Finally, our calculated absolute quasiparticle band-edge energies are summarized in Fig. 4 (a), in which the DFT results are also listed for reference. The enhanced many-electron interactions in monolayer dichalcogenides substantially changes the absolute band-edge energy from the DFT results. However, the general trend of the evolution of the band-edge energies are similar for both DFT and GW results. For instance, the band-edge energy of MX_2 gradually increases as X varies from S to Te or M varies from Mo to W. A particularly interesting point is that the self-energy corrections modify both valence band and conduction band-edge energies similarly, as seen from Fig. 4 (a). This is substantially different from the corrections found by previous HFT studies, in which the corrections mainly affect the VBM [22].

The band alignments in Fig. 4 exhibit several unusual features. First, even after the costly GW calculation, except the $\text{WSe}_2/\text{WTe}_2$ interface, the qualitative types of band alignments for these materials from DFT and HFT/HSE have not changed. For example, all of these calculations consistently predict that the interface of MoS_2 and MoSe_2 has a type II (staggered) band alignment. Secondly, the values of GW-calculated band offsets are larger than those from DFT or HFT, mainly due to larger bandgap corrections. Therefore, a sophisticated calculation, such as the GW method, may be necessary in order to obtain

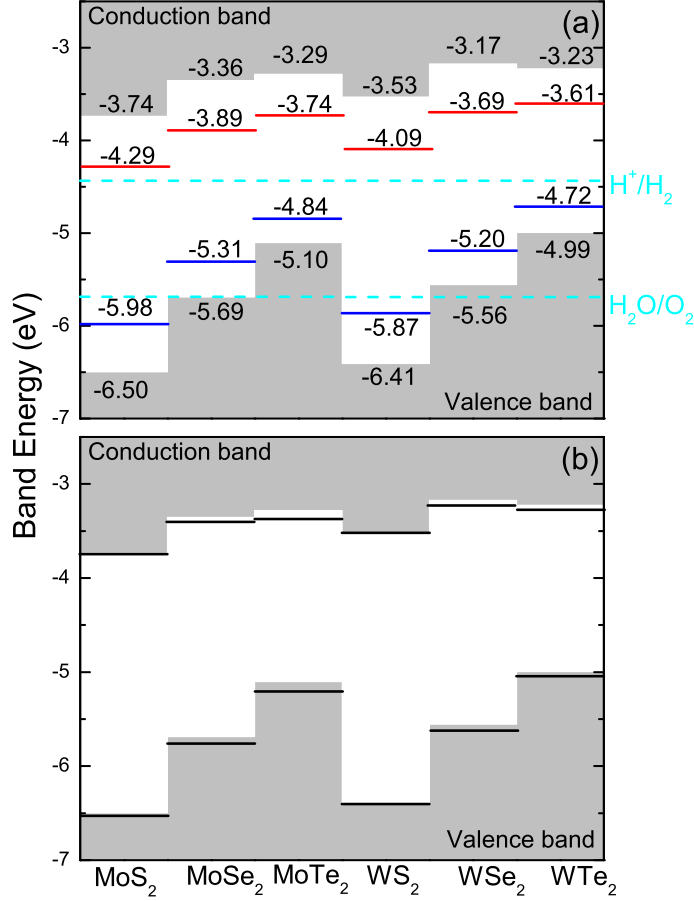


FIG. 4: (Color online) The absolute band-edge energy of calculated monolayer dichalcogenides relative to the vacuum level to the vacuum level. (a) The blue and red dashed lines stand for the DFT/PBE results while the grey-shadow regions stand for the GW results. The water reduction (H^+/H_2) and oxidation (H_2O/O_2) are marked by the cyan dashed lines, respectively. (b) The absolute band-edge energies by the fully converged GW simulation (grey-shadow regions) and the band-gap-center approximation (solid dark lines).

the quantitative band offset for heterojunctions of 2D chalcogenides, while DFT or HFT calculation can be convenient when assessing the type of the band alignment or other properties [32]. On the other hand, for heterojunctions of our studied 2D chalcogenides with other semiconductors, our calculated absolute band-edge energy shall be crucial to decide the band offsets and even alignments.

Earlier work predicts that monolayer MoS₂ and WS₂ may work for water splitting [22]. Hereby we have marked the energy levels for the oxidation and reduction processes of water

splitting in Fig. 4 (a). The GW calculation yields a similar conclusion although the VBMs are usually lower and the CBMs are generally higher than those of DFT and HFT results.

Previously, in order to avoid the slowly converging absolute band energy, the band-gap-center approximation was proposed to estimate the absolute band-edge energy with the assumption that the self-energy correction shifts both CBM and VBM by similar amounts but in inverse directions [23, 26]. Interestingly, we find this model works very well for our studied monolayer dichalcogenides. As shown in Fig. 4 (b), the band-gap-center approximation gives nearly the same band-edge energy as the costly direct GW calculation. As discussed above, the reason for this agreement is that our converged GW calculation yields similar corrections for both the DFT-calculated VBM and CBM. Therefore, this band-gap-center approximation may be particularly useful for estimating the band offset of 2D dichalcogenides because it only requires the quasiparticle bandgap.

One must be cautious when applying our absolute band-edge energy towards realistic applications. Here we only consider the isolated monolayer structures surrounded by vacuum. However, for realistic conditions, the environmental effects will be extremely important for these ultra-thin layer of semiconductors. For example, the background dielectric response may substantially reduce the self-energy corrections, affecting the band gap and band offset dramatically [24, 35]. Moreover, for photocatalytic processes, such as water splitting, excitonic effects must be included since such processes are driven by optically-excited excitons. In particular, electron-hole (e - h) interactions are known to be enhanced in monolayer chalcogenides and in many other reduced-dimensional semiconductors [15, 34]. Thus e - h interactions will substantially reduce the energy of the optical absorption edge, making it significantly different from the quasiparticle bandgap. In this sense, more sophisticated calculations including the environment effects and the impact of excitons are desirable, which is a major thrust in the field nanotechnologies as well. However, our calculation serves as a valuable foundation for such studies.

In conclusion, we have employed a first-principles GW calculation to obtain the quasiparticle band structure and absolute band-edge energy of monolayer dichalcogenides. Our converged GW simulation not only produces the bandgaps but also provides the band offsets of relevant heterojunctions. Both the bandgap and absolute band-edge energy are substantially different from previous DFT and HFT/HSE results. Surprisingly, the band-gap-center model works very well for obtaining the absolute band-edge energy without a fully-converged

GW simulation, making it a convenient way to estimate the band offsets and chemical activity of monolayer dichalcogenides.

We acknowledge the support by NSF Grant No. DMR-1207141. The computational resources have been provided by Lonestar of Teragrid at the Texas Advanced Computing Center (TACC). The ground state calculation is performed by the Quantum Espresso [36]. The GW calculation is done with the BerkeleyGW package[37].

-
- [1] K.S. Novoselov, D. Jiang, F. Schedin, T.J. Booth, V.V. Khotkevich, S.V. Morozov, and A. K. Geim, Proc. Natl. Acad. Sci. U.S.A 102, 10451 (2005).
 - [2] K. Mak, C. Lee, J. Hone, J. Shan, and T. F. Heinz, Phys. Rev. Lett. 105, 136805 (2010).
 - [3] A. Splendiani, L. Sun, Y. Zhang, T. Li, J. Kim, C.-Y. Chim, G. Galli and F. Wang, Nano Lett. 10, 1271 (2010).
 - [4] B. Radisavljevic, A. Radenovic, J. Brivio, V. Giacometti, and A. Kis, Nat. Nanotechnol. 6, 147 (2011).
 - [5] Y. Li, Z. Zhou, S. Zhang, and Z. Chen, J. Am. Chem. Soc. 130, 16739 (2008).
 - [6] W. Chen, E.J.G. Santos, W. Zhu, E. Kaxiras, and Z. Zhang, Nano Lett. 13, 509514 (2013).
 - [7] B. Hinnemann, P.G. Moses, J. Bonde, K.P. Jrgensen, J.H. Nielsen, S. Horch, I. Chorkendorff, J.K. Nrskov, J. Am. Chem. Soc. 127, 5308 (2005).
 - [8] T.F. Jaramillo, K.P. Jrgensen, J. Bonde, J.H. Nielsen, S. Horch, I. Chorkendorff, Science 317, 100 (2007).
 - [9] Y. Li, H. Wang, L. Xie, Y. Liang, G. Hong, and H. Dai, J Am Chem Soc. 133, 7296 (2011).
 - [10] D. Xiao, G.-B. Liu, W. Feng, X. Xu, and W. Yao, Phys. Rev. Lett. 108, 196802 (2012).
 - [11] T. Cao, G. Wang, W. Han, H. Ye, C. Zhu, J. Shi, Q. Niu, P. Tan, E. Wang, B. Liu, and J. Feng, Nat. Communications 3, 887 (2012).
 - [12] K.F. Mak, K. He, J. Shan, and T. F. Heinz, Nat. Nanotechnology 7, 494 (2012).
 - [13] H. Zeng, J. Dai, W. Yao, D. Xiao, and X. Cui, Nat. Nanotechnology 7, 490493 (2012).
 - [14] J. Heyd, G. E. Scuseria, and M. Ernzerhof, J. Chem. Phys. 118, 8207 (2003).
 - [15] A. Ramasubramaniam, Phys. Rev. B 86, 115409 (2012).
 - [16] T. Cheiwchanchamnangij and W.R.L. Lambrecht, Phys. Rev. B 85, 205302 (2012).
 - [17] H.-P. Komsa and A.V. Krashennnikov, Phys. Rev. 86, 241201 (2012).

- [18] F. Bernardini and V. Fiorentini, Phys. Rev. B 57, 9427 (1998).
- [19] C.G. Van de Walle and R.M. Martin, Phys. Rev. B 35, 81548165 (1987).
- [20] S.-H. Wei and A. Zunger, Appl. Phys. Lett. 72, 2011 (1998).
- [21] Y. Nishibayashi, K. Segawa, J. D. Singh, S.-I. Fukuzawa, K. Ohe, and S. Uemura, Organometallics 15, 370 (1996).
- [22] J. Kang, S. Tongay, J. Zhou, J. Li, and J. Wu, Appl. Phys. Lett. 102, 012111 (2013)
- [23] H. Jiang, J. Phys. Chem. C 116, 7664 (2012).
- [24] X. Blase, C. Attaccalite, and V. Olevano, Phys. Rev. B 83, 115103 (2011).
- [25] W. Kang, M. S. Hybertsen, Phys. Rev. B 82, 085203 (2010).
- [26] M.C. Toroker, D.K. Kanan, N. Alidoust, L.Y. Isseroff, P. Liao, and E.A. Carter, Phys. Chem. Chem. Phys. 13, 16644 (2011).
- [27] J. P. Perdew, K. Burke, and M. Ernzerhof, Phys. Rev. Lett. 77, 3865 (1996).
- [28] N. Troullier and J.L. Martins, Phys. Rev. B **43**, 1993 (1991).
- [29] M.S. Hybertsen and S.G. Louie, Phys. Rev. B **34**, 5390 (1986).
- [30] C.D. Spataru, S. Ismail-Beigi, L.X. Benedict, and S.G. Louie, Phys. Rev. Lett. **92**, 077402 (2004).
- [31] B. Arnaud, S. Lebgue, P. Rabiller, and M. Alouani, Phys. Rev. Lett. **96**, 026402 (2006).
- [32] A. Kormanyos, V. Zolyomi, N.D. Drummond, P. Rakytá, G. Burkard, and V.I. Falko, arXiv:1304.4084v2 (2013).
- [33] L. Yang, C.-H. Park, Y.-W. Son, M.L. Cohen, and S.G. Louie, Phys. Rev. Lett. **99**, 186801 (2007).
- [34] L. Yang, Phys. Rev. B **83**, 085405 (2011).
- [35] J.B. Neaton, M.S. Hybertsen, and S.G. Louie, Phys. Rev. Lett. 97, 216405 (2006).
- [36] P. Giannozzi, S. Baroni, N. Bonini, M. Calandra, R. Car, C. Cavazzoni, D. Ceresoli, G.L. Chiarotti, M. Cococcioni and I. Dabo, *et al.*, J.Phys.:Condens.Matter, **21**, 395502 (2009).
- [37] J. Deslippe, G. Samsonidze, D.A. Strubbe, M. Jain, M.L. Cohen, and S.G. Louie, Comput. Phys. Commun. **183**, 1269 (2012).